Journal of the European Ceramic Society 22 (2002) 1137–1148

www.elsevier.com/locate/jeurceramsoc

# Microhardness anisotropy and the indentation size effect on the basal plane of single crystal hematite

Michael E. Stevenson[a,c], Masaki Kaji[b], Richard C. Bradt[c,*]

[a]*QORE Inc., Materials Engineering Division, 1039 Industrial Court, Suwanee, GA 30024, USA*
[b]*Kyocera Corporation, Central Research Laboratory, 1-4 Yamashita-cho, Kagoshima, 899-43, Japan*
[c]*Metallurgical and Materials Engineering, The University of Alabama, A-129 Bevill Research Building, Tuscaloosa, AL 35487-0202, USA*

Received 8 May 2001; accepted 23 July 2001

**Abstract**

The Knoop microhardness anisotropy of single crystal hematite, $Fe_2O_3$, was investigated on the basal plane (0001) at indentation test loads from 50 to 1000 g. Microhardness maxima were observed for low indentation test loads when the long axis of the Knoop indenter was parallel to the $<2\bar{1}\bar{1}0>$. Microhardness minima occurred for the $<10\bar{1}0>$ orientations. The microhardness anisotropy at low indentation test loads is associated with slip dominance on the primary slip system of the corundum structure, the $\{0001\}<11\bar{2}0>$. An energy balance was applied to the indentation size effect (ISE) and also to address the microhardness anisotropy. The load independent, orientation independent, Knoop microhardness for the basal plane is 5.35 GPa. The ISE was further investigated by lubrication of the specimen test surface just prior to the Knoop microindentation process. Results from the lubricated microhardness tests are compared with the standard dry Knoop microhardness test results and reveal a significant reduction in the ISE. This indicates that friction between the test specimen and the indenter facets is a major contribution to the ISE. 

*Keywords:* Anisotropy; Crystals; $Fe_2O_3$; Hardness; Indentation

## 1. Introduction

Indentation hardness testing is widely used to describe numerous material parameters for a variety of research and development endeavors.[1–5] There are three levels or scales of indentation hardness measurements: the nano, the micro, and the macro. The first two scales correspond to their prefixes. Nanohardness indentations are on the sub-micron scale. They have proven to be of value in estimating the mechanical properties of very fine scale structures including precipitates and thin films. The Berkovich triangular pyramidal indenter has been popular for those studies, however, spherical indenters are also becoming of interest.[6] Microbardness indentations are of the micron size scale and have been extensively applied at the microstructural level. Knoop or Vickers diamond pyramid indenters are usually applied to these microhardness measurements. Macrohardness measurements are much larger in scale, often applied as bulk testing procedures. Macrohardness results are often correlated with the mechanical properties of the material as a whole, including the yield strength and tensile strength. A number of techniques are associated with macrohardness testing, the most popular of which are the Rockwell and the Brinell hardness measurements. When applied to ceramics, unfortunately, macrohardness testing usually results in massive cracking.

Two important phenomena have been documented to occur during the microhardness testing of single crystal ceramic specimens. These are: (i) microhardness anisotropy[1,7] and (ii) the indentation size effect (ISE).[8,9] Relative to the anisotropy, indentation microhardnesses have been documented to be a function of both the crystal plane and the crystallographic direction on that plane. The single crystal microhardness anisotropy has been explained by reference to the primary slip system for the particular crystal structure of interest. Researchers have reported and explained the presence of microhardness anisotropy in many different crystal structures, including the BCC metals, FCC metals, $Al_2O_3$ (corundum or

* Corresponding author.
*E-mail address:* rcbradt@coe.eng.ua.edu (R.C. Bradt).

0955-2219/02/$ - see front matter 
PII: S0955-2219(01)00415-0

sapphire), NaCl (rock salt), diamond cubic materials and $CaF_2$ (fluorite).[1,7,10–12]

The ISE is the increase of apparent microhardness with a decrease of the indentation test load. It is sometimes conversely stated as the decrease of microhardness with an increase in the applied indentation test load. This phenomenon has been documented to extend into the nanohardness regime.[6,8] It is usually represented by plotting the microhardness as a function of either the indentation test load, or the resulting indentation impression size. The ISE is illustrated schematically in Fig. 1. The apparent microhardness is a function of the test load for low indentation test loads, where there is no single value for the microhardness. At high indentation test loads, the microhardness is constant with respect to the indentation test load and a single, well defined hardness value exists. It is the load independent hardness, $H_{LIH}$, a quantity that has also been referred to as the "true" hardness in some of the literature.

There exists a natural interest in the mechanical properties of hematite, $Fe_2O_3$, a compound that is isostructural with sapphire ($Al_2O_3$). This oxide of iron is an important ore for steelmaking, is widely used in magnetic recording media, is an important polishing compound (rouge) and is used for the color in some industrial pigments. In the applications as a polishing compound, hardness is particularly important. This paper reports a study of the Knoop microhardness of natural hematite single crystals on the basal (0001) plane. The microhardness anisotropy and the ISE on this crystal plane are addressed and explained.

## 2. Experimental procedures

Natural single crystals of hematite, $Fe_2O_3$, were obtained from the ore pile of USIMINAS in Ipatinga, Minas Gerais, Brazil. These crystals were flat hexagonal shapes approximately 5 mm thick and 3 cm across the flats. The nominal purity of these crystals was determined using energy dispersive X-ray analysis (EDAX) in a scanning electron microscope. Only Fe and O were detected. X-ray diffraction confirmed the corundum structure. Specimens of these single crystals were prepared for microhardness measurements using a diamond saw to cut basal plane (0001) test specimens. Oriented samples were mounted in Bakelite and manually polished through 600-grit silicon carbide. Final polishing was completed with a 1 μm $\alpha$-$Al_2O_3$ followed by a 0.05 μm $\gamma$-$Al_2O_3$ in an automatic vibratory polisher for 48 h to achieve a scratch-free, mirror-like finish.

Microhardnesses were measured using a Buehler Micromet 2004 automated testing machine fitted with a Knoop indenter and adapted with a goniometer stage for precise definition of the angular orientation of the test specimen. The Knoop indenter geometry was chosen because it provides a long, shallow pyramidal indentation with essentially no elastic relaxation and a very low

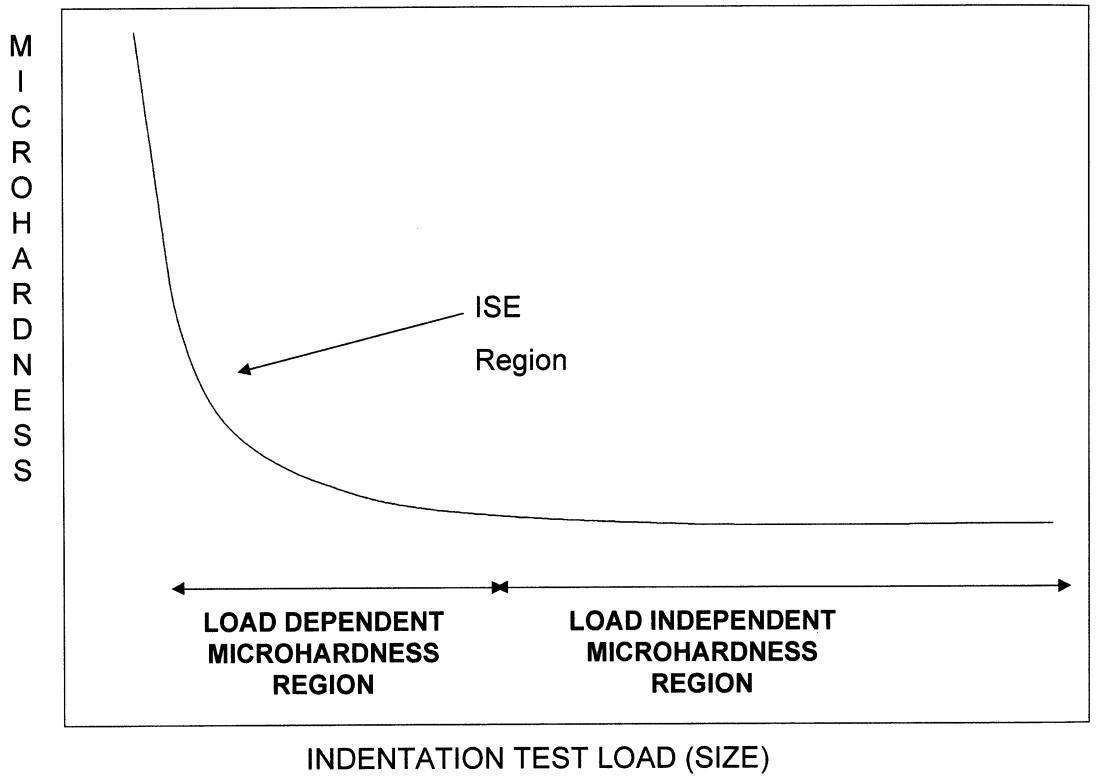


Fig. 1. Microhardness variation with test load showing the indentation size effect.

propensity for cracking.[13] The Knoop indenter geometry provides an excellent means to study the microhardness anisotropy of a material by orienting the long axis of the indenter parallel to specific crystallographic directions. That is the directional specification in this study. Knoop microhardnesses were determined from the equation:

$$H_K = \frac{14.229 \cdot P}{d^2} \quad (1)$$

where $P$ is the applied indentation test load and $d$ is the length of the long axis of the resulting pyramidal shaped indentation. The impression diagonal length was measured immediately after indentation and converted to a Knoop microhardness number by Eq. (1).

To observe the complete symmetry of the basal plane, Knoop microhardness measurements were taken from the $[2\bar{1}\bar{1}0]$ to the $[\bar{1}2\bar{1}0]$ on the (0001). To assess the indentation size effect, the ISE, Knoop microhardnesses were taken at the following five different indentation test loads: 50, 100, 200, 500 and 1000 g. A dwell time of 10 s was used for all of the microhardness measurements. Indentations with obvious cracks were not used in the microhardness compilations, as cracked indentations have been demonstrated to yield spurious microhardness results.[14] However, as hematite is relatively soft and the Knoop indenter creates a long, shallow impression, cracked indentations were rare. Ten symmetrical, well defined indentations were obtained for each test condition. Microhardness averages are reported with their 95% confidence intervals based on the "$t$" distribution.

In addition to the Knoop microhardness measurements made on the as-polished hematite, additional measurements were made with the specimen surface lubricated. This was accomplished by applying a standard SAE 10W–30W motor oil to the polished test specimen surface with a cotton swab. After application of the lubricant, Knoop microhardness measurements were completed for only the $[2\bar{1}\bar{1}0]$ and $[10\bar{1}0]$ directions. The same number of indentations were completed at each indentation test load in parallel to the microhardness measurements on the unlubricated hematite single crystal. Direct comparisons of the dry and lubricated Knoop microhardnesses were then completed.

## 3. Results and discussion

For the (0001) plane, the microhardnesses as a function of crystallographic orientation from the $[2\bar{1}\bar{1}0]$ to the $[\bar{1}2\bar{1}0]$ for each indentation test load are shown in Fig. 2. Here, it should be noted that 1000 kg mm$^{-2}$ is 9.81 GPa. These results clearly illustrate the microhardness anisotropy, the variation of microhardness with crystallographic direction on the basal plane. For the (0001) basal plane, microhardness maxima are observed at low indentation test loads when the long axis of the Knoop indenter is aligned parallel to the $<2\bar{1}\bar{1}0>$ directions. Microhardness minima occur for the $<10\bar{1}0>$ orientations. These maxima and minima are in exactly the same orientations as reported for alumina or corundum ($Al_2O_3$) by O'Neill.[1] It is also apparent that the degree, or extent of the observed crystalline microhardness anisotropy decreases with increasing indentation test load. It is significant that the directional microhardness anisotropy is practically non-existent for the 1000 g indentation test load.

The Knoop microhardness results in Fig. 2 also reveal the ISE. Microhardness values that are obtained for the lower indentation test loads are considerably higher than those for the larger indentation test loads. This observation is best illustrated by the form of representation in Fig. 3, which presents the load dependence of the microhardness on the basal plane similar to the schematic in Fig. 1. The Knoop microhardness values at the 500 and 1000 g indentation test loads appear to be approaching a load independent hardness, $H_{\mathrm{LIH}}$, as previously described.

### 3.1. Energy balance

As reviewed by Quinn and Quinn,[15] different approaches have been applied to explain microhardness results. One of the first to apply energy methods to indentation hardness measurements were Wonsiewicz and Chin.[16] Their work was based on the strain energy of plastic deformation and the relation of the hardness anisotropy to the operative slip systems in the test material. More recently an energy balance approach has also been applied by Nowak and Sakai.[17] Their definition of the "true" hardness differs somewhat from the traditional concept. Because of the merits of those two previous studies, the results of this study are also analyzed through an energy balance. The results of that approach to conventional microhardness measurements yields a relationship including the indentation test load and the resulting indentation diagonal length.[18] That relationship is of the form:

$$\frac{P}{d} = a_1 + a_2 \cdot d. \quad (2)$$

Eq. (2) can be directly applied as a regression equation to estimate the microbardness parameters $a_1$ and $a_2$. That process only requires a series of indentation test loads and the resulting indentation sizes, microhardness data such as that presented in Fig. 3.

By applying the regression analysis of Eq. (2), the load independent Knoop microhardness, $H_{\text{K-LIH}}$, is then obtained from:

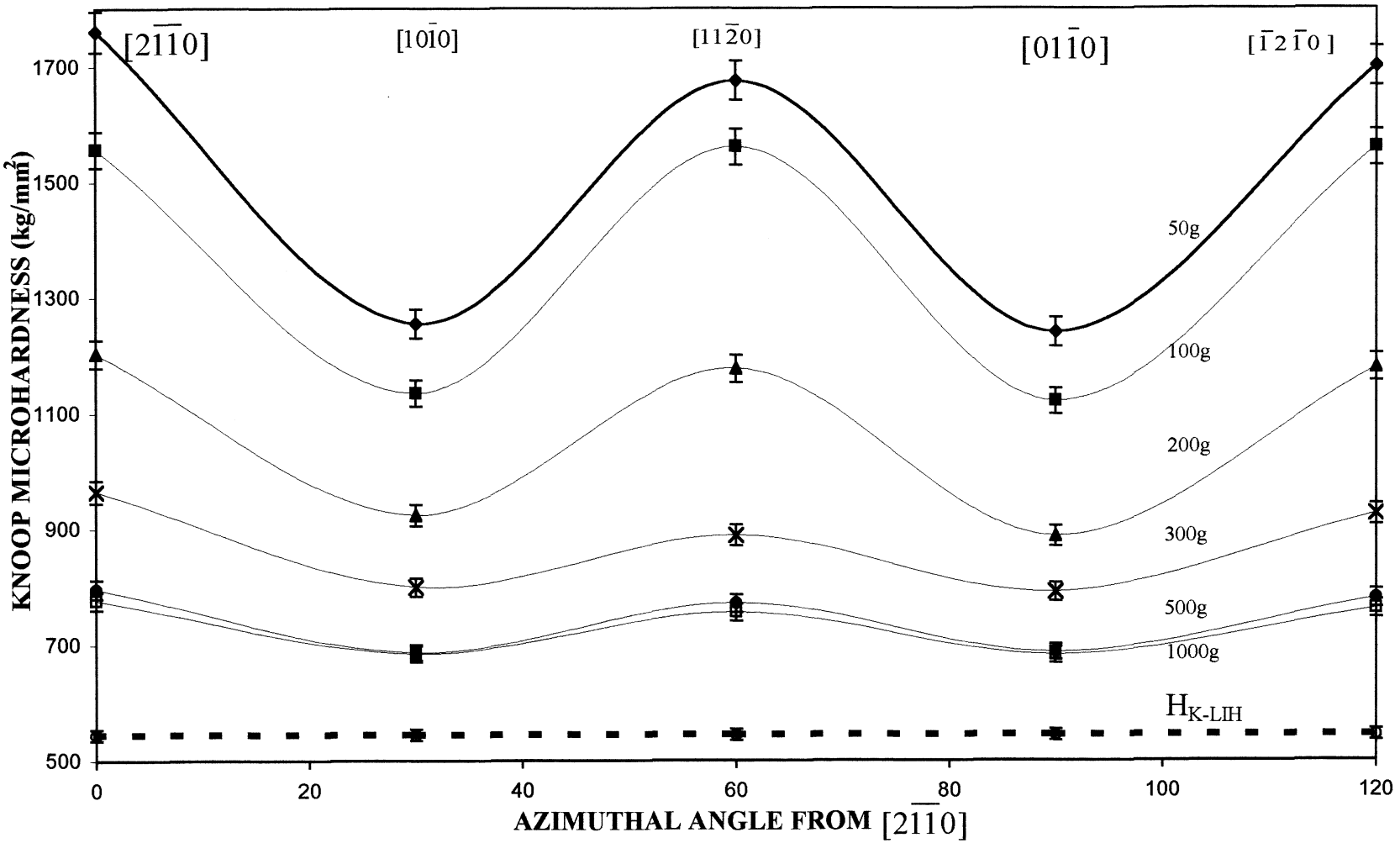


Fig. 2. Knoop microhardness of hematite on the basal plane, the (0001), and its variation with crystallographic orientation and indentation test load.

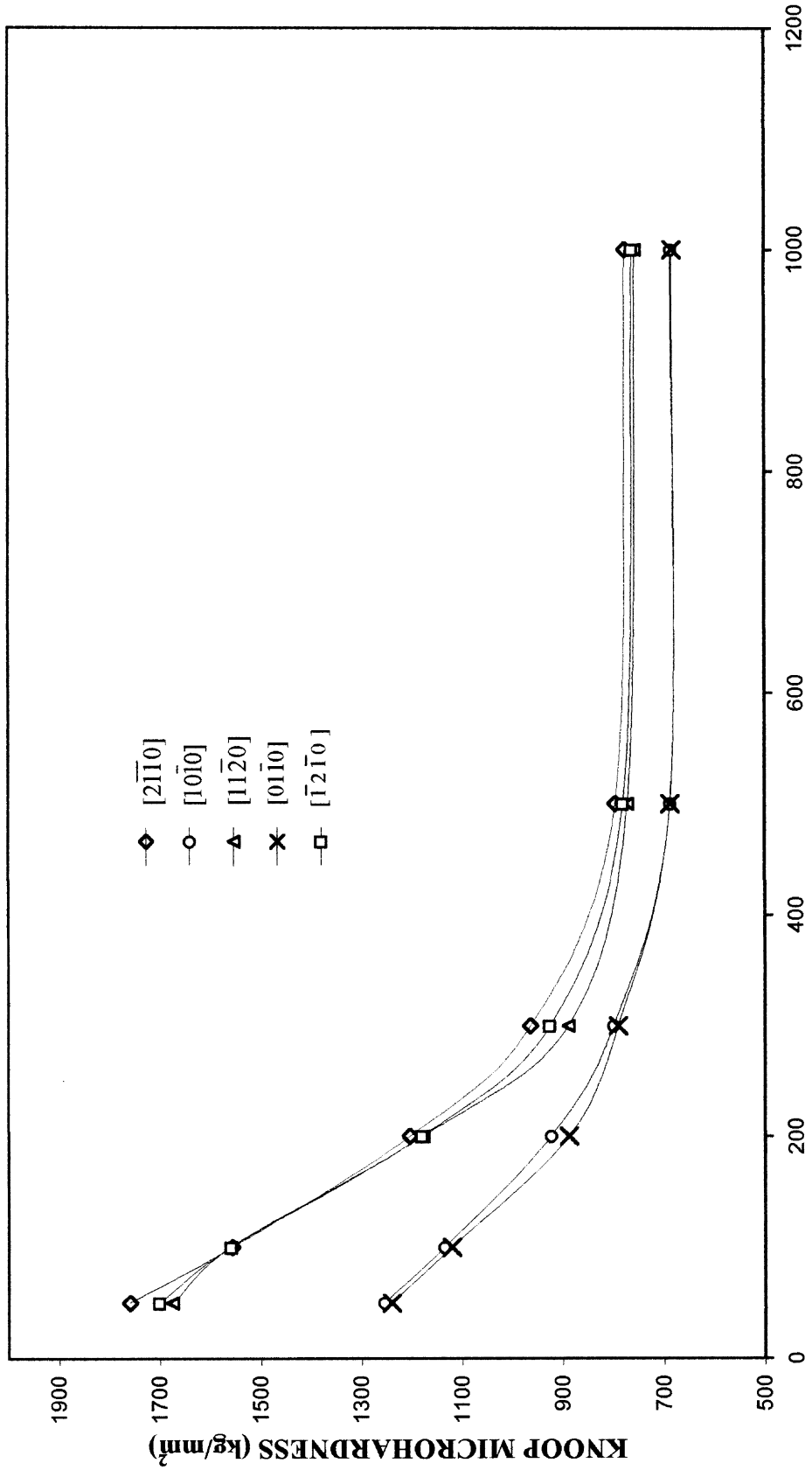


Fig. 3. Load dependence of the microhardness of hematite.

$$H_{\mathrm{LIH}} \approx 14.229 \cdot a_2 \quad (3)$$

This form is identical to the relationship discussed by Kaji et al.[19] The $a_2$ value has been previously referred to as the characteristic hardness of the material by Frischat in his studies of glass.[20] By combining the term for the load independent microhardness, $a_2$, with the Knoop microhardness constant, 14.229, from Eq. (1), it is possible to determine the load independent Knoop microhardness. All that is required is a set of data taken over a range of loads such as the results that are presented in Figs. 2 and 3 for the hematite single crystals.

Values of $a_1$, $a_2$, and $H_{\mathrm{K\text{-}LIH}}$ are determined through a linear regression analysis between the experimental values for $(P/d)$ and $(d)$. The complete procedure requires that this regression be performed for each orientation on each crystal plane for the entire range of indentation test loads. Representative plots of this regression analysis are shown in Fig. 4. Correlation coefficients indicate that there is a high level of confidence to the fit of the experimental data to this model. Results for all of the measured orientations are summarized in Table 1.

Once the load independent Knoop microhardnesses have been determined, a combined representation of the Knoop microhardness can be made. The load independent Knoop microhardness is presented as the heavy dashed line in the lower portion of Fig. 2. It is evident that the load independent Knoop microhardnesses, the $H_{\mathrm{K\text{-}LIH}}$, is not a function of the crystallographic direction on the basal plane of hematite. This is particularly significant, as the low indentation test load Knoop microhardnesses, which have distinct maxima and minima at different orientations, all converge to the same load independent hardness value at high indentation test loads. The extent of Knoop microhardness anisotropy gradually decreases as the indentation test load is increased. Eventually, at high indentation test loads, the basal plane Knoop microhardness is isotropic. Combining all of the results yields a basal plane $H_{\mathrm{K\text{-}LIH}}$ of $545 \pm 9.4$ kg/mm$^2$.

### 3.2. The microhardness of hematite

Applying the previous concepts to determine the load independent Knoop microhardnesses for hematite allows for a comparison with other published hardness values for hematite. The $H_{\mathrm{K\text{-}LIH}}$ is $545 \pm 9.4$ kg/mm$^2$ ($5.35 \pm 0.1$ GPa) for the basal (0001) plane. The mineralogical text by Zoltai and Stout[28] reports a Mohs hardness from 5.5 to 6.5 for hematite. Converting these values to the Knoop microhardness scale yields a range from about 450 to 700 kg/mm$^2$. This range of values is in satisfactory agreement with the load independent hardnesses measured in this study.

Only the Vickers indentation microhardness data of Kollenberg[21] appears to have been reported for single crystal hematite. Kollenberg reported the Vickers microhardnesses for the basal plane to be 1000 kg/mm$^2$ at room temperature for a single indentation test load of 200 g. This result compares favorably with the Knoop microhardnesses of about 1200 kg/mm$^2$ on the basal plane at the 200 g test loads in this study. Since Kollenberg did not present microhardness data as a function of indentation test load, the role that the ISE may have assumed in the Vickers microhardness measurements by Kollenberg cannot be ascertained. However, with respect to the microhardness data obtained at similar indentation test loads, the Knoop microhardness data obtained in this study does compare favorably with the Vickers results published by Kollenberg. The results presented here also compare favorably with the mineral hardness estimation for hematite presented by Szymanski and Szymanski.[22]

Table 1
Regression analysis summary of the Knoop microhardness on the basal plane

| Orientation | $a_1$ (kg/mm) | $a_2$ (kg/mm$^2$) | $H_{\mathrm{K\text{-}LIH}}$ (kg/mm$^2$) | $R^2$ |
|---|---|---|---|---|
| $[2\bar{1}\bar{1}0](0001)$ | $1.94 \pm 0.09$ | $39.14 \pm 0.72$ | $557 \pm 10.2$ | 0.98 |
| $[10\bar{1}0](0001)$ | $1.34 \pm 0.06$ | $37.93 \pm 0.58$ | $540 \pm 8.7$ | 0.99 |
| $[11\bar{2}0]$ (0001) | $1.90 \pm 0.08$ | $37.90 \pm 0.75$ | $539 \pm 10.7$ | 0.97 |
| $[01\bar{1}0]$ (0001) | $1.29 \pm 0.06$ | $38.19 \pm 0.53$ | $543 \pm 7.5$ | 0.99 |
| $[\bar{1}2\bar{1}0]$ (0001) | $1.91 \pm 0.08$ | $38.22 \pm 0.73$ | $545 \pm 10.4$ | 0.98 |

### 3.3. Microhardness anisotropy at low indentation test loads

Fig. 2 illustrates significant directional microhardness anisotropy for hematite on the basal (0001) plane, but only at the lower indentation test loads. Since the classic paper of Daniels and Dunn[7] nearly a half century ago, this type of variation of microhardness with direction on a specific crystallographic plane has been satisfactorily explained for many different crystal structures by an effective resolved shear stress model.[1,23] From the geometry of the indenter and the applied indentation test load, the resolved shear stress on the primary slip system is calculated and shown to be a minimum for those indenter orientations that yield the hardness maxima and a maximum for those orientations of the hardness minima. Brookes and Burnand[23] have applied this model to alumina which also has the corundum crystal structure, the same structure as hematite. They concluded that the (0001) $<11\bar{2}0>$ primary slip system is expected to produce the microhardness anisotropy which is observed and reported for the low indentation test loads in Fig. 2.

There do not appear to have been any extensive studies directed specifically to the slip process in hematite, $Fe_2O_3$. However, several publications addressing rhombohedral twinning in hematite, namely those of Bursil

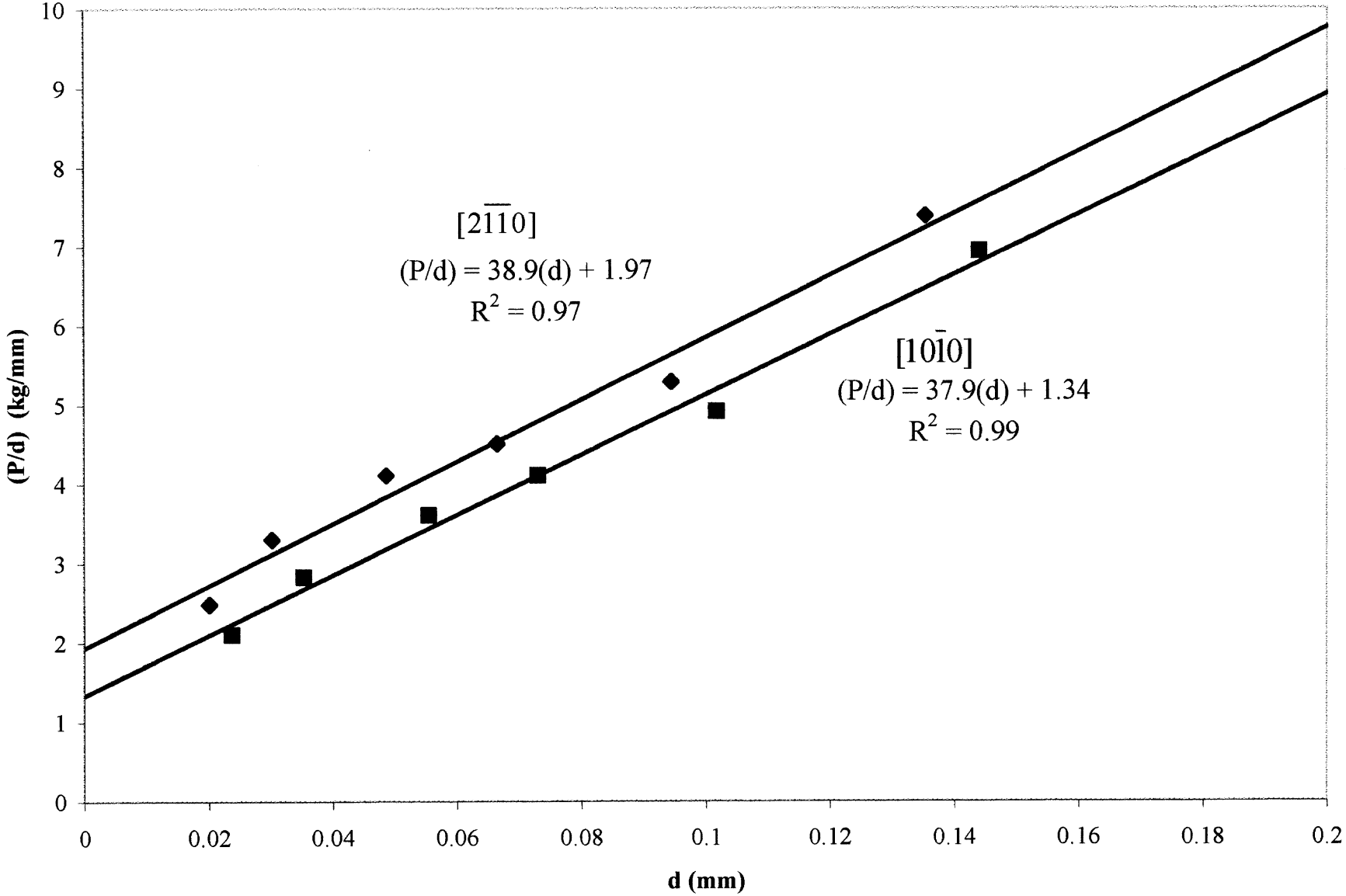


Fig. 4. Energy balance regression analysis for the dry and lubricated microhardnesses in the [2$\bar{1}\bar{1}$0] on the (0001) of hematite.

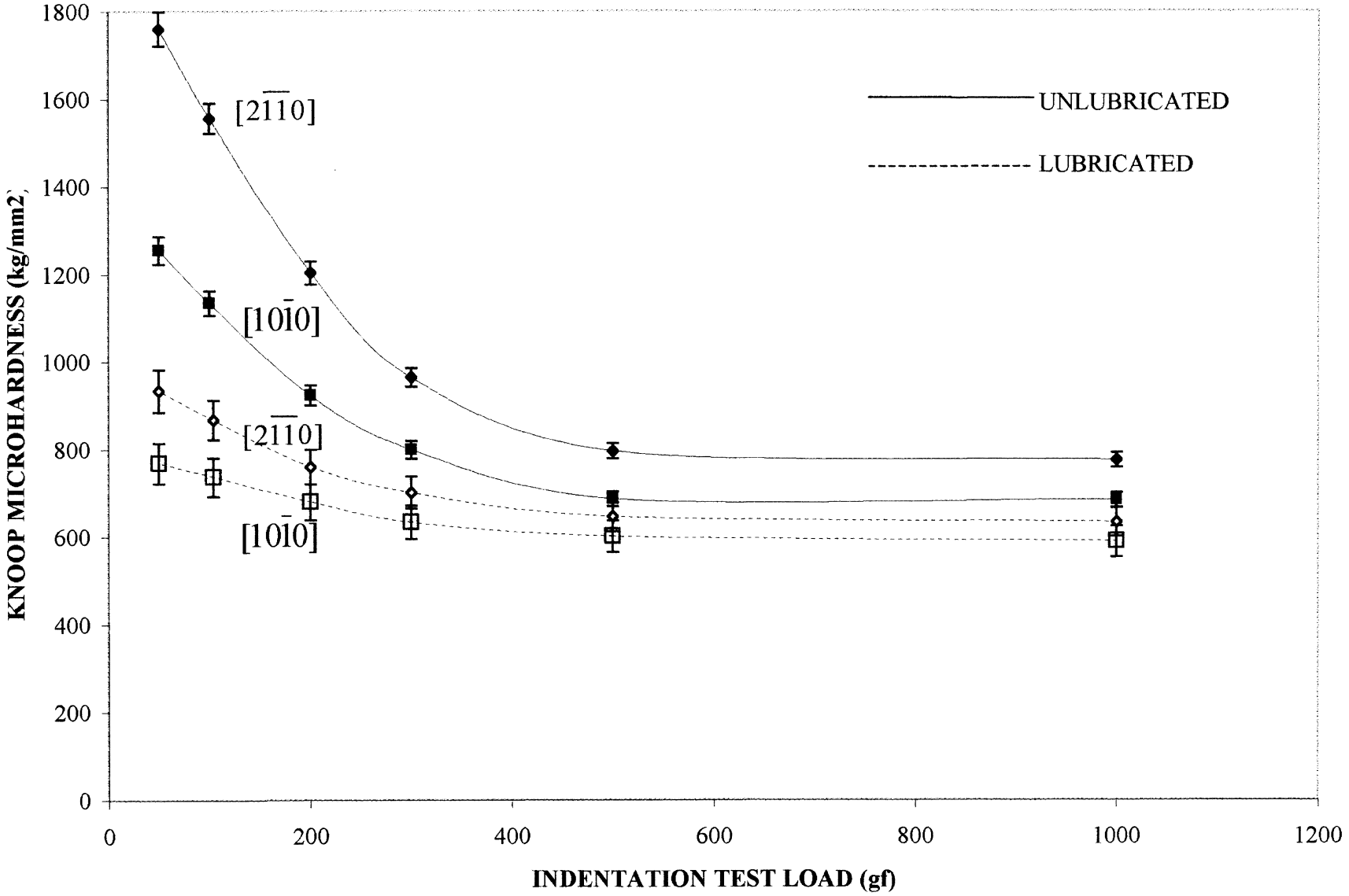


Fig. 5. Energy balance regression analysis for [2$\bar{1}$10] and [10$\bar{1}$0] on the (0001) of hematite.

and co-workers[24] and Geipel et al.,[25] suggest that the same slip systems are active in hematite, $Fe_2O_3$, as are active in alumina, $Al_2O_3$. This is not surprising as both possess the corundum crystal structure, and differ only very slightly in lattice parameters. Single crystal alumina exhibits the same Knoop microhardness anisotropy on the basal plane, as previously reported by Brookes and Burnand[23] and that microhardness anisotropy is directly attributable to (0001) $<11\bar{2}0>$ slip. It must be concluded that the low indentation test load Knoop microhardness anisotropy for hematite, as illustrated in Fig. 2, is also the consequence of deformation dominated by the primary slip system, the (0001) $<11\bar{2}0>$ of the corundum structure.

### 3.4. The indentation size effect

It is necessary to address the ISE and specifically, how it reduces the measured microhardness with increasing test load. It is evident that as the indentation test load increases, the indentations become larger and the volume of flowed material about the indentation must also increase to accommodate this situation. This necessitates the activation of multiple slip systems to account for the increased volume of plastically deformed material. The activation of multiple slip systems is expected to significantly increase the dislocation density in the immediate vicinity of the indentation. It might be expected that this would create extensive work hardening in the vicinity of an indentation, which in turn would be expected to increase the measured microhardness. However, instead of a microhardness increase from a work hardening process, the measured Knoop microbardness decreases significantly, from about 1300 kg/mm$^2$ to less than 700 kg/mm$^2$. This is approximately a 50% reduction in the apparent Knoop microhardness on the (0001) plane.

Obviously the ISE is not a work hardening phenomenon related to dislocation processes in the vicinity of an indentation. Ma and Clarke[26] and Nix and Gao[6] do present a plausible explanation of a dislocation mechanism on the basis of geometric and statistical dislocations within the concept of strain gradient plasticity. Nevertheless, however appealing a dislocation process explanation of the ISE may be, the role of any dislocation phenomena must be seriously questioned. Supporting the non-dislocational nature of the ISE is the fact that an ISE has also been reported in amorphous glasses,[20,27,28] as well as for single crystals and polycrystals.[17,27] It is necessary to address the characteristics of the indentation itself for an explanation of the ISE for dislocation phenomena are not a universal explanation.

In contrast to the dislocation based theories for the ISE, others have identified the interactions at the interface, or surface between the indenter facets and the test specimen to provide an explanation for the ISE.[28,29] A proportional specimen resistance model, based on a force balance was proposed by Li and Bradt[30] and it has been applied to address the role of friction between the specimen surface and the indenter facets on the ISE. That research points to the geometry of the Knoop indenter and the surface area to volume ratio ($\alpha$ $1/d$) of the indentation as the critical factor. Complementary to the argument that the ISE is governed by surface frictional effects between the specimen and the indenter facets, Shi and Atkinson[29] and Bystrzycki and Varin[31] have independently demonstrated that for lubricated specimen surfaces, the ISE is decreased. More recently, Kaji et al.[19] have also confirmed the role of friction by lubricating microhardness measurements on the basal plane of single crystal alumina. It is because of the results of these studies that the lubricated microhardness measurements of hematite described in the experimental procedures were completed.

Fig. 5 illustrates those lubricated microhardness results for the $[2\bar{1}\bar{1}0]$ and $[10\bar{1}0]$ indenter orientations. From these results it is obvious that the application of a lubricating agent during the indentation process significantly decreases the magnitude or presence of the ISE and the measured Knoop microhardness values as well. In identical fashion to the analysis performed for the dry microhardness measurements, the lubricated load independent Knoop microhardnesses were addressed by applying a regression analysis between ($P/d$) and ($d$). This form of analysis is illustrated for the lubricated Knoop microhardness measurements in Fig. 6 for the $[2\bar{1}\bar{1}0]$. Note that the two lines are parallel. The quantitative results of the energy balance analysis are presented in Table 2.

From the summary in Table 2 and the results of Fig. 6, it is evident that the $a_2$ parameter, and consequently the load independent Knoop micro hardness, $H_{\text{K-LIH}}$, do not change significantly in the presence of a lubricating agent. By contrast, the $a_1$ parameter, asserted to be a measure of surface effects during indentation, is decreased by more than a factor of two in the presence of the lubricant. This result confirms the role of the $a_1$ constant as a measure of the surface effects during indentation. It also directly relates it to the ISE. Additionally, the fact that the load independent Knoop microhardnesses do not change significantly in the presence of the lubricant substantiates the application of the energy balance approach as a

Table 2
Summary of the dry and lubricated regression analysis results

| Orientation | $a_1$ (kg/mm) | $a_2$ (kg/mm$^2$) | $H_{\text{K-LIH}}$ (kg/mm$^2$) | $R^2$ |
|---|---|---|---|---|
| $[2\bar{1}\bar{1}0]$(0001) Unlubricated | 1.94±0.09 | 39.14±0.72 | 557±10.2 | 0.98 |
| $[2\bar{1}\bar{1}0]$ (0001) Lubricated | 0.82±0.08 | 38.73±1.03 | 551±14.3 | 0.99 |
| $[10\bar{1}0]$ (0001) Unlubricated | 1.34±0.06 | 37.93±0.58 | 540±8.7 | 0.99 |
| $[10\bar{1}0]$ (0001) Lubricated | 0.57±0.05 | 37.64±0.94 | 536±12.7 | 0.99 |

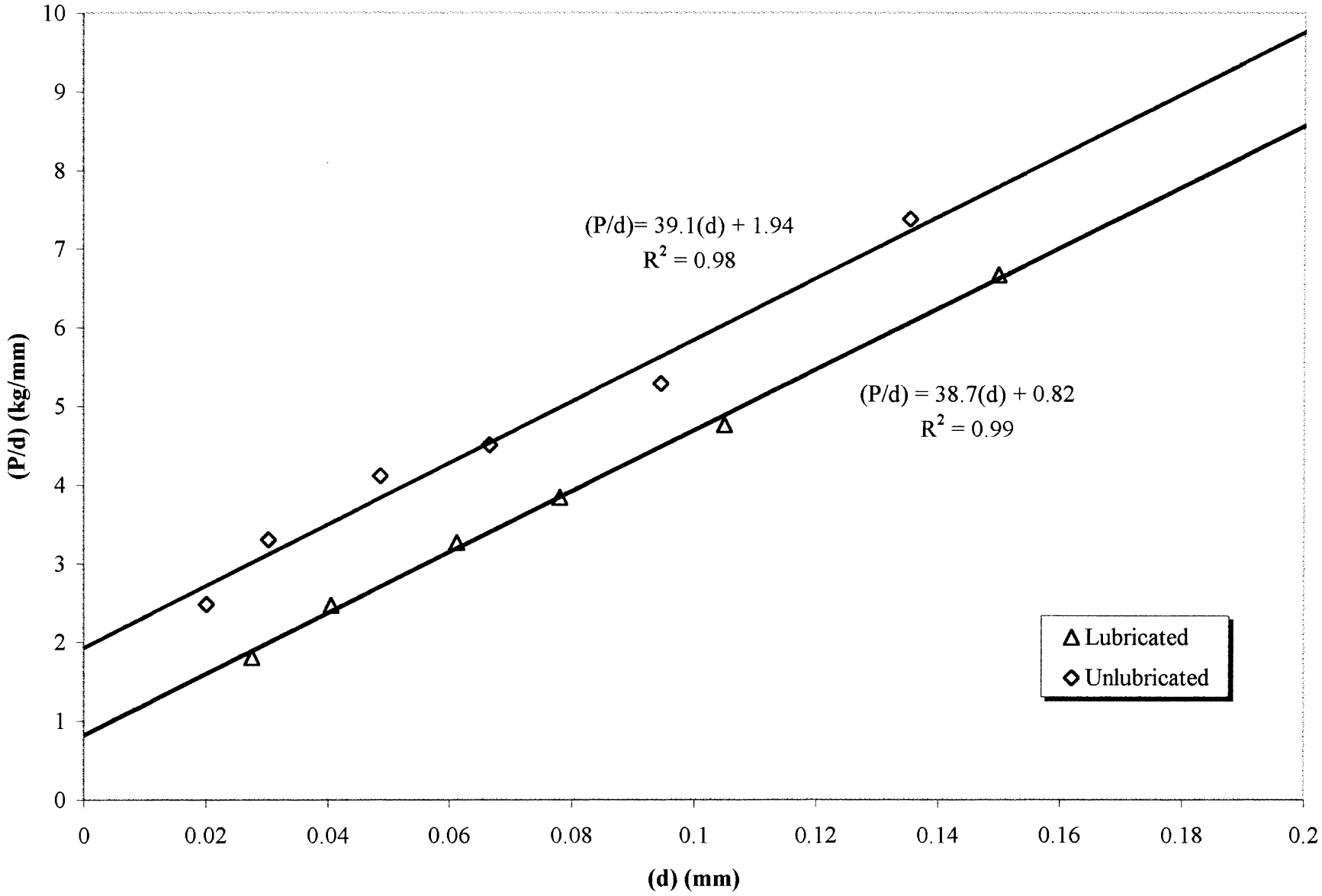


Fig. 6. Comparison of the dry and lubricated microhardnesses in the $[2\bar{1}\bar{1}0]$ and $[10\bar{1}0]$ on the (0001) of hematite.

means to estimate the microhardness of a material independent of the test environment. From these results, it must be concluded that friction between the indenter and the test specimen contributes significantly to the presence of the ISE. Additional experiments are necessary to determine the amount or percentage of that contribution.

A comparison can also be made between the results of this study and the similar experimental results of Kaji et al.[19] for single crystal sapphire. That study addressed the ISE and microhardness anisotropy for both lubricated and unlubricated Knoop microbardness measurements on the basal plane specimens of single crystal alumina (sapphire). From a qualitative standpoint, there are several parallel results between this study and the results of Kaji et al.[19] With regards to the microhardness anisotropy, both studies observed maxima in the $<2\bar{1}\bar{1}0>$ and minima in the $<10\bar{1}0>$, the same as reported by Brookes and coworkers. This is expected for both have the same primary slip systems. Additionally, the trend of decreasing anisotropy with increasing indentation test load is observed in both cases. Interesting comparisons occur when examining the lubricated vs. unlubricated results. Kaji et al.[19] report a decrease of nearly 30% for the $<2\bar{1}\bar{1}0>$ at an indentation test load of 50 gf. In parallel, for the same orientation and indentation test load, the decrease in hardness for hematite is almost 40%. Additionally, both studies report that the load independent Knoop microhardnesses, the $H_{\text{K-LIH}}$, are identical for both the lubricated and unlubricated test conditions. Of course, the values for the $H_{\text{K-LIH}}$ are considerably higher for the alumina ($\sim$1150 kg/mm$^2$ vs. $\sim$550 kg/mm$^2$ for hematite), which is to be expected if one considers the higher elastic modulus and the Mohs hardness values for alumina relative to those of hematite.

## 4. Summary and conclusions

Knoop microbardnesses were measured on the (0001) plane of single crystal hematite for a range of indentation test loads and indentation orientations. At low test loads, microhardness maxima were observed for the Knoop indenter aligned parallel to the $<2\bar{1}\bar{1}0>$ directions and minima for the $<10\bar{1}0>$. As the indentation test load is increased, the degree of the microhardness anisotropy decreases significantly. This trend is attributable to the activation of multiple slip systems for the larger indentations corresponding to higher indentation test loads. When multiple slip systems are activated, the directional specificity of the domination by the primary slip system is lost.

In addition to studying the microhardness anisotropy, the indentation size effect was also examined through the comparison of dry and lubricated microhardness measurements. It was observed that lubrication during testing significantly reduces the presence of the ISE, indicating that friction between the indenter facets and the test specimen constitutes a significant portion of the ISE. This is particularly true at low indentation test loads where the surface area to volume ratio of the impression is high. For both the lubricated and unlubricated experiments, the load independent, orientation independent Knoop microhardness for the basal plane of hematite, $Fe_2O_3$ was determined to be $5.35 \pm 0.1$ GPa.

## References


1. O'Neill, J. B., Brookes, C. A. and Redfern, B. A., Anisotropy in the hardness of single crystals. *Proceedings of the Royal Society of London*, 1971, **322**, 73–88.
2. McColm, I. J., *Ceramic Hardness*. Plenum, New York, 1990 (pp. 178–180).
3. O'Neill, H., *The Hardness of Metals and its Measurement*. Sherwood, Cleveland, OH, 1934.
4. Lawn, B. R. and Blau, P. J., *ASTMSTP 889: Microindentation Techniques in Materials Science and Engineering*. ASTM, Philadelphia, PA, 1986 (pp. 1–11).
5. Westbrook, J., Shaw, J. and Conrad, H., *The Science of Hardness Testing and its Research Applications*. ASM, Metals Park, OH, 1973 (pp. 1–3).
6. Nix, W. D. and Gao, H., Indentation size effects in crystalline materials: a law for strain-gradient plasticity. *Journal of the Mechanics and Physics of Solids*, 1998, **46**, 411–425.
7. Daniels, F. W. and Dunn, C. G., The effect of orientation on Knoop hardness of single crystals of zinc and silicon ferrite. *Transactions of ASMI*, 1949, **41**, 419–422.
8. Swain, M. and Bradt, R. C., Nano and micro hardnesses of single crystal yttrium aluminum garnet (YAG) on the (111) plane. In *1995 Snowbird Conference on Deformation of Ceramics*. Plenum, 1995, pp. 195–206.
9. Tate, D. R., A comparison of microhardness indentation tests. *Transactions of ASM*, 1945, **35**, 374–375.
10. Garfinkle, M. and Garlick, R. G., A stereographic representation of Knoop microhardness anisotropy. *Transactions of AIME*, 1968, **242**, 809–814.
11. Busovne, B. J., Kotchick, D. M. and Tressler, R. E., Deformation history effects on the precipitation behavior of $Ti^{4+}$ doped sapphire. *Philosophical Magazine A*, 1979, **39**, 265–276.
12. Li, H., Suematsu, H., Iseki, T. and Bradt, R. C., Microhardness anisotropy and the indentation load/size effect in MgO–$Al_2O_3$ single crystals. *Nippon Serrmikkusu Kyobai Gakujutsu Ronbunshi*, 1991, **99**, 1079–1087.
13. Sakai, M., Shimzu, S. and Ishikawa, T., The indentation load-depth curve of ceramics. *Journal of Materials Research*, 1999, **14**, 1471–1484.
14. Li, H. and Bradt, R. C., The effect of indentation induced cracking on the apparent microhardness. *Journal of Materials Science*, 1996, **31**, 1065–1070.
15. Quinn, J. B. and Quinn, G. D., Indentation brittleness of ceramics: a fresh approach. *Journal of Materials Science*, 1997, **32**, 4331–4346.
16. Wonsiewicz, B. C. and Chin, G. Y., A theory of Knoop hardness anisotropy. In *The Science of Hardness Testing and its Research Applications*, ed. J. Westbrook, J. Shaw and H. Conrad. ASM, Metals Park, OH, 1973, pp. 167–173.
17. Nowak, R. and Sakai, M., Energy principle of indentation contact: the application to ceramics. *Journal of Materials Research*, 1993, **8**, 1068–1078.
18. Stevenson, M. E. and Bradt, R. C., Analysis of microhardness measurements. *Advanced Materials and Processes: Heat Treating Progress*, 2000, **158**(2), H41–H43.

19. Kaji, M., Stevenson, M. E. and Bradt, R. C., Knoop microhardness anisotropy and the indentation size effect of the basal plane of single crystal alumina (sapphire). Submitted to *J. Am. Ceram. Soc.*
20. Frischat, G. H., In *Strength of Inorganic Glass*, ed. C. R. Kurkjian. Plenum, New York, 1985, pp. 135–140.
21. Kollenberg, W., Microhardness measurement of haematite single crystals at temperatures up to 900 °C. *Journal of Materials Science*, 1986, **21**, 4310–4314.
22. Szymanski, A. and Szymanski, J. M., *Hardness Estimation of Minerals, Rocks and Ceramic Materials*. Elsevier, New York, 1989 (pp. 44–45).
23. Brookes, C. A. and Bumand, R. P., Hardness anisotropy in crystalline solids. In *The Science of Hardness Testing and its Research Applications*, ed. J. Westbrook, J. Shaw and H. Conrad. ASM, Metals Park, OH, 1973, pp. 199–211.
24. Bursill, L., Julin, P. and XuDong, F., Rhombohedral twin structure in haemetite. *Australian Journal of Chemistry*, 1992, **45**, 1527–1546.
25. Geipel, T., Lagerlof, K., Pirouz, P. and Heuer, A., A zonal dislocation mechanism for rhombohedral twinning elements of haemetite. *Acta Materialia*, 1994, **42**, 1367–1372.
26. Ma, Q. and Clarke, D. R., Size dependent hardness of silver single crystals. *Journal of Materials Research*, 1995, **10**, 853–862.
27. Li, H. and Bradt, R. C., The indentation load size effect and the measurement of the hardness of vitreous silica. *Journal of Non Crystalline Solids*, 1991, **146**, 197–212.
28. Hirao, K. and Tomozawa, M., Microhardness of $SiO_2$ glass in various environments. *Journal of the American Ceramic Society*, 1987, **70**, 497–502.
29. Shi, H. and Atkinson, M., A friction effect in low-load hardness testing of copper and aluminum. *Journal of Materials Science*, 1991, **25**.
30. Li, H. and Bradt, R. C., Knoop microhardness anisotropy of single crystal $LaB_6$. *Materials Science and Engineering A*, 1991, **142**, 51–61.
31. Bystrzycki, J. and Varin, R. A., The frictional component in microhardness testing of intermetallics. *Scripta Metallurgica et Materiala*, 1993, **29**, 605–609.